

Gaussian-Process-based Robot Learning from Demonstration

Miguel Arduengo¹, Adrià Colomé¹, Joan Lobo-Prat¹, Luis Sentis² and Carme Torras¹

Abstract—Endowed with higher levels of autonomy, robots are required to perform increasingly complex manipulation tasks. Learning from demonstration is arising as a promising paradigm for easily extending robot capabilities so that they adapt to unseen scenarios. We present a novel Gaussian-Process-based approach for learning manipulation skills from observations of a human teacher. This probabilistic representation allows to generalize over multiple demonstrations, and encode uncertainty variability along the different phases of the task. In this paper, we address how Gaussian Processes can be used to effectively learn a policy from trajectories in task space. We also present a method to efficiently adapt the policy to fulfill new requirements, and to modulate the robot behavior as a function of task uncertainty. This approach is illustrated through a real-world application using the TIAGo robot.

I. INTRODUCTION

In the context of robotics, learning from demonstration (LfD) is the paradigm in which robots learn a task policy from examples provided by a human teacher. This facilitates non-expert robot programming and enables robots to move away from repeating simple predefined behaviors and toward learning to take actions in unstructured environments.

Trajectory-based methods are a well-established approach to learn movement policies in robotics [1]. These methods encode skills by extracting trajectory patterns from the available demonstrations (Figure 1). A probabilistic representation is often adopted, as it allows to encode the variability of the learned trajectory. The demonstrated trajectories are assumed to represent samples of an underlying stochastic process, and thus reproductions are obtained by sampling the learned distribution over trajectories [2].

Several approaches such as Gaussian Mixture Regression (GMR) [3,4], Dynamic Movement Primitives (DMP) [5,6] and Probabilistic Movement Primitives (ProMP) [7,8] have been extensively studied in the literature. These representations have proved successful at learning and generalizing the desired trajectories in various scenarios. However, each representation has its limitations. Due to an explicit description of the trajectory dynamics, DMP introduces many open parameters in addition to basis functions and their weighting coefficients. The same problem arises in ProMP, where basis functions have to be manually defined. In order to alleviate the modeling of trajectories via specific functions, GMR has been employed to model the distribution of demonstrated motions. Despite the improvements with respect to other techniques, adapting learned skills with GMR is not straightforward [9].



Fig. 1. The proposed Gaussian-Process-based learning from demonstration approach allows to teach the robot manipulation tasks such as opening doors.

In recent years, there has been a growing interest in Gaussian Processes [10,11]. One can think of a Gaussian Process (GP) as defining a distribution over functions, and inference taking place directly in the space of functions [12]. Unlike GMR, which provides a generative model, GP provides a discriminative model. In practice, generative models require less data, but their generalization performance is often poorer than that of discriminative models [13]. In trajectory learning applications, GP is a more suitable representation for modulating the learned policy than GMR.

A few works have studied the use of Gaussian Process representation in the LfD context [14,15]. Among the most representative is the one presented by Schneider et al. [16]. They propose a representation of a pick-and-place task that effectively encodes the skill uncertainty. However, they do not address the adaptation of the policy. In a recent work, Jaquier et al. [17] propose a novel multi-output GP based on GMR for encoding a trajectory. They take advantage of the ability of GP to encode prior beliefs through the mean and kernel functions and the capability of GMR to make predictions far from training data. Nevertheless, the improvement with respect to standard GMR comes at the cost of an increasing complexity with respect to standard GP. Neither of these works considers the representation of rotations, required for modelling a trajectory in task space.

In this work, we present a general Gaussian-Process-based learning from demonstration approach. We show how to achieve an effective representation of the manipulation skill, inferred from the demonstrated trajectories. We address the adaptation of the policy through via-points, and the modulation of the robot behavior depending on the task uncertainty. The remainder of this paper is structured as follows: in Section II we discuss the theoretical aspects of the considered GP models; in Section III we present the proposed learning from demonstration framework; in Section IV we illustrate the main aspects of the paper through a real-world application; in Section V we summarize the conclusions.

¹Institut de Robotica i Informàtica Industrial (IRI), Barcelona, Spain. {marduengo, acolome, jlobo, torras}@iri.upc.edu

²Human Centered Robotics Laboratory (HCRL), UT Austin, USA. lsentis@austin.utexas.edu

II. GAUSSIAN PROCESS MODELS

In this section we discuss the theoretical background of the proposed LfD approach. First, we present the fundamentals of GP. Then, we address the challenges of modeling rigid-body dynamics with them. Finally, we present how heteroscedastic GP allows to accurately represent the uncertainty of the taught manipulation task.

A. Gaussian Process Fundamentals

Intuitively, a Gaussian Process can be seen as a distribution over functions. Conditioning our prior belief of this distribution on the training data we can obtain a model that explains the observations. Formally, a GP is a collection of random variables, any finite number of which have a joint Gaussian distribution [18]. It can be completely specified by its mean function $m(t)$ and covariance or kernel function $k(t, t')$:

$$m(t) = \mathbb{E}[f(t)] \quad (1)$$

$$k(t, t') = \mathbb{E}[(f(t) - m(t))(f(t') - m(t'))] \quad (2)$$

where $f(t)$ is the underlying stochastic process, $m(t)$ depicts the prior knowledge of its mean, and the specification of $k(t, t')$ implies an a-priori distribution over functions. We are interested in incorporating the knowledge that the training data $\mathcal{D} = \{(t_i, y_i)\}_{i=1}^N$ provides about $f(t)$. We consider that we do not have available direct observations, but only noisy versions y . Let $\mathbf{m}(t)$ be the vector of the mean function evaluated at all training points t and $K(t, t^*)$ be the matrix of the covariances evaluated at all pairs of training and prediction points t^* . Assuming additive independent identically distributed Gaussian noise with variance σ_n^2 , we can write the joint distribution of the observed target values \mathbf{y} and the function values at the test locations \mathbf{f}^* under the prior as:

$$\begin{bmatrix} \mathbf{y} \\ \mathbf{f}^* \end{bmatrix} \sim \mathcal{N} \left(\begin{bmatrix} \mathbf{m}(t) \\ \mathbf{m}(t^*) \end{bmatrix}, \begin{bmatrix} K(t, t) + \sigma_n^2 I & K(t, t^*) \\ K(t^*, t) & K(t^*, t^*) \end{bmatrix} \right) \quad (3)$$

The posterior distribution over functions can be computed by conditioning the joint Gaussian prior distribution on the observations $p(\mathbf{f}^* | t, \mathbf{y}, t^*) \sim \mathcal{N}(\mu^*, \Sigma^*)$ where:

$$\mu^* = \mathbf{m}(t^*) + K(t^*, t) [K(t, t) + \sigma_n^2 I]^{-1} [\mathbf{y} - \mathbf{m}(t)] \quad (4)$$

$$\Sigma^* = K(t^*, t^*) - K(t^*, t) [K(t, t) + \sigma_n^2 I]^{-1} K(t, t^*) \quad (5)$$

When we consider only the prediction of one output variable, $k(t, t')$ is a scalar function. The previous concepts can be extended to multiple-output GP (MOGP) by taking a matrix covariance function $\mathbf{k}(t, t')$. Usual approaches to MOGP modelling are mostly formulated around the Linear Model of Coregionalization (LMC) [19]. For a d -dimensional output the kernel is expressed in the following form:

$$\mathbf{B} \otimes \mathbf{k}(t, t') = \begin{bmatrix} B_{11}k_{11}(t_1, t'_1) & \dots & B_{1d}k_{1d}(t_1, t'_d) \\ \vdots & \ddots & \vdots \\ B_{d1}k_{d1}(t_d, t'_1) & \dots & B_{dd}k_{dd}(t_d, t'_d) \end{bmatrix} \quad (6)$$

where $\mathbf{B} \in \mathbb{R}^{d \times d}$ is regarded as the coregionalization matrix and t_i represents the input corresponding to the i -th output.

Diagonal elements correspond to the single-output case, while the off-diagonal elements represent the prior assumption on the covariance of two different output dimensions [20]. If no a-priori assumption is made, $B_{ij} = 0$ for $i \neq j$ and the MOGP is equivalent to d independent GP.

Regarding the form of $k(t, t')$, typically kernel families have free hyperparameters Θ . Such parameters can be determined by maximizing the log marginal likelihood:

$$\log p(\mathbf{y} | t, \Theta) = -\frac{1}{2} \mathbf{y}^T K_y^{-1} \mathbf{y} - \frac{1}{2} \log |K_y| - \frac{N}{2} \log 2\pi \quad (7)$$

where $K_y = K(t, t) + \sigma_n^2 I$. This optimization problem might suffer from multiple local optima.

B. Rigid-Body Motion Representation

In the LfD context, representation of trajectories in task space is usually required. A drawback of GP is that it requires an Euclidean vector space structure on the output space. For this reason, the modelling of rotations is not straightforward, since they do not have an Euclidean representation. A common approach is to use the Euler angles. However, when rotations are large this might result in inaccurate predictions. Rotations can also be represented by a set of unit length Euler axes \mathbf{u} together with a rotation angle θ :

$$SO(3) \subset \{\theta \mathbf{u} \in \mathbb{R}^3 / \|\mathbf{u}\| = 1 \wedge \theta \in [0, \pi]\} \quad (8)$$

where $SO(3)$ denotes the rotation group. This set defines the solid ball $B_\pi(0)$ in \mathbb{R}^3 with radius $0 \leq r \leq \pi$ which is closed, dense and compact. Ambiguity in the representation occurs for $\theta = \pi$. To obtain an isomorphism between the rotation group $SO(3)$ and the axis-angle representation, we can fix the axis representation for $\theta = \pi$:

$$\tilde{B}_\pi(0) = B_\pi(0) \setminus \{\pi \mathbf{u} / u_z < 0 \vee (u_z = 0 \wedge u_y < 0) \vee (u_z = u_y = 0 \wedge u_x < 0)\} \quad (9)$$

where $\mathbf{u} = (u_x, u_y, u_z)$. This parametrization is a minimal and unique $SO(3) \simeq \tilde{B}_\pi(0)$. Rigid motion dynamics is given by a mapping from time to translation and rotation $h: \mathbb{R} \rightarrow SE(3)$. Let the translational components be defined by the Euclidean vector $\mathbf{v} \in \mathbb{R}^3$. Then $SE(3)$ is defined isomorphically by $SE(3) \simeq \mathbb{R}^3 \times \tilde{B}_\pi(0)$. Thus, rigid body motion can be represented in MOGP with the 6-dimensional output vector structure $(\mathbf{v}, \theta \mathbf{u}) = (x, y, z, \theta u_x, \theta u_y, \theta u_z)$.

Another possible, more accurate representation, can be achieved with dual quaternions [21]. However, as shown in [22], with the proposed parametrization, a good performance is attained and computations are more efficient.

C. Heteroscedastic Gaussian Process

The standard Gaussian Process model assumes a constant noise level. This can be an important limitation when encoding a manipulation task. Consider the example shown in Figure 2: it is evident that while the initial and final positions are highly constrained, that is not the case for the path to follow between such positions. In graphs a) and b) we can see that with a standard approach we accurately represent the mean but not the variability of demonstrations.

Considering an independent normally distributed noise, $\lambda \sim \mathcal{N}(0, r(t))$, where the variance is input-dependent and modeled by $r(t)$. The mean and covariance of the predictive distribution can be modified to:

$$\mu^* = \mathbf{m}(t^*) + K(t^*, t) [K(t, t) + R(t)]^{-1} [\mathbf{y} - \mathbf{m}(t)] \quad (10)$$

$$\Sigma^* = K(t^*, t^*) + R(t^*) - K(t^*, t) [K(t, t) + R(t)]^{-1} K(t, t^*) \quad (11)$$

where $R(t)$ is a diagonal matrix, with elements $r(t)$.

Taking into account the input-dependent noise shown in Figure 2d) the uncertainty in the different phases of the manipulation task is effectively encoded by the uncertainty of Figure 2c). This approach is commonly referred to as heteroscedastic Gaussian Process [23].

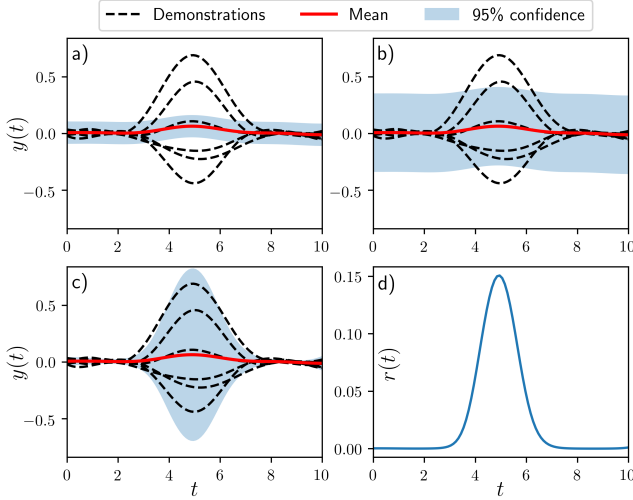


Fig. 2. Standard GP does not accurately model the uncertainty of the demonstrated task as can be seen in a) and b), where it is underestimated and overestimated, respectively. On the other hand, the heteroscedastic GP approach, in c), adequately encodes the uncertainty in the different phases of the task, considering the local noise in d).

III. LEARNING FROM DEMONSTRATION FRAMEWORK

In this section, we present the proposed GP-based LfD framework. First, we formalize the problem of learning manipulation skills from demonstrated trajectories. Then, we propose an approach for encoding the learned policy with GP. Next, we discuss the temporal alignment of demonstrations. We also present a method that allows to adapt the learned policy through via-points. Finally, we study how the uncertainty model of GP can be exploited to stably modulate the robot behavior, varying end-effector virtual dynamics.

A. Problem Statement

In LfD we assume that a dataset of demonstrations is available. In the trajectory-learning case, the dataset consists of a set of trajectories \mathbf{s}_i together with a timestamp $t_i \in \mathbb{R}$, $\mathcal{D} = \{(t_i, \mathbf{s}_i)\}_{i=1}^N$. Without loss of generality, we will consider $\mathbf{s}_i \in SE(3)$. The aim is to learn a policy π that infers, for a given time, the desired end-effector pose \mathbf{s}_i^d to perform the taught manipulation task: $\mathbf{s}_i^d = \pi(t_i)$. The policy must generate continuous and smooth paths, and generalize over multiple demonstrations.

B. Manipulation Task Representation with GP

Representing a manipulation task using heteroscedastic GP models requires the specification of $m(t)$, $k(t, t')$ and $r(t)$. As we have discussed in Section II-B, a suitable mapping for representing a trajectory is given by the following MOGP:

$$\pi(t) \sim \mathcal{GP}(\mu^*, \Sigma^*) : t \longrightarrow (x, y, z, \theta u_x, \theta u_y, \theta u_z) \quad (12)$$

The prior mean function is commonly defined as $m(t) = 0$. Although not necessary in general, if no prior knowledge is available this is a simplifying assumption. The GP covariance function controls the policy function shape. The chosen kernel must generate continuous and smooth paths. Note also that the time parametrization of trajectories is invariant to translations in the time domain. Thus, the covariance function must be stationary. That is, it should be a function of $\tau = t - t'$. The Radial Basis Function (RBF) kernel fulfils all these requirements:

$$k(t, t') = \sigma_f^2 \exp\left(-\frac{[t - t']^2}{2l^2}\right) \quad (13)$$

with hyperparameters l and σ_f . Moreover, for multidimensional outputs, we have to consider the prior interaction. In the general case, we usually do not have any previous knowledge about how the different components of the demonstrated trajectories relate to each other. Thus, we can assume that the 6 components are independent a-priori. The matrix covariance function can then be written as:

$$\mathbf{k}(t, t') = \text{diag}\left(\sigma_{f1}^2 e^{([t-t']^2/l_1^2)}, \dots, \sigma_{f6}^2 e^{([t-t']^2/l_6^2)}\right) \quad (14)$$

where $\text{diag}()$ refers to diagonal, and l_i and σ_{fi} correspond to output dimension i . In Section II-C we discussed the convenience of specifying an input-dependent noise function $r(t)$ for encoding the manipulation skill with GP. Usually, it is not known a-priori and must be inferred from the demonstrations. As proposed in [24], first a standard GP can be fit to the data. Its predictions can be used to estimate the input-dependent noise empirically. Then, a second independent GP can be used to model $z(t) = \log[r(t)]$. Let \mathcal{Z} be the set of noise data $\mathbf{z} = \{z_i\}_{i=1}^n$ and its predictions \mathbf{z}^* . The posterior predictive distribution can be approximated by:

$$p(\mathbf{f}^* | \mathcal{D}, t^*) = \iint p(\mathbf{f}^* | \mathcal{D}, \mathcal{Z}, t^*) p(\mathcal{Z} | \mathcal{D}, t^*) \simeq p(\mathbf{f}^* | \mathcal{D}, \mathcal{Z}, t^*) \quad (15)$$

where $\mathcal{Z} = \arg \max_{\mathbf{z}, \mathbf{z}^*} p(\mathbf{z}, \mathbf{z}^* | \mathcal{D}, t^*)$. Therefore, we have specified all the required functions of the model.

C. Temporal Alignment of Demonstrations

For inferring a time dependent policy, the correlation between the temporal and spatial coordinates of two demonstrations of the same trajectory must remain constant. In general, it is very difficult for a human to repeat them at the same velocity. Thus, a time distortion appears (Figure 2a), and should be adequately corrected. Dynamic Time Warping (DTW) [25,26] is a well-known algorithm for finding the optimal match between two temporal sequences, which may vary in speed.

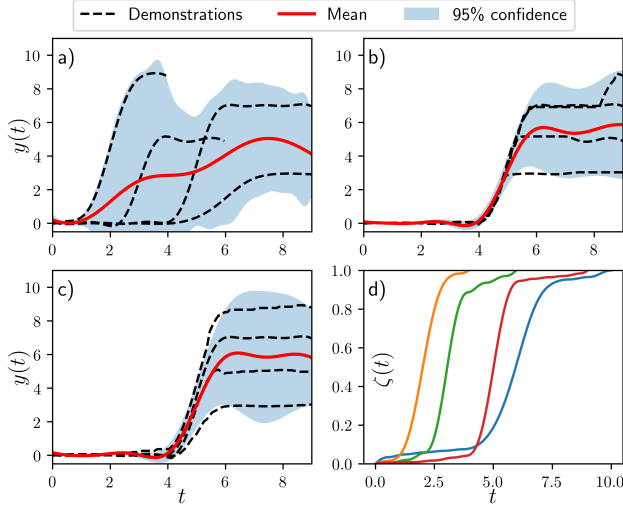


Fig. 3. In a) we observe that due to distortion in time, task constraints are not encoded correctly. In b) the trajectories are aligned with DTW using the Euclidean distance as similarity measure. In c) we show the resulting alignment using the proposed TCI d), as similarity measure.

The algorithm finds a non-linear mapping of the demonstrated trajectories and a reference based on a similarity measure. A common measure among the existing LfD frameworks is the Euclidean distance [27]. This relies on the assumption that the manipulation task can be performed always following the same path. For instance, consider the case of a pick-and-place task where the objects have to be placed in shelves at different levels. Using the Euclidean distance as similarity measure will lead to an erroneous temporal alignment (Figure 2b), since intermediate points for placing the object at a higher level can be mapped to ending points of a lower level. We propose to use an index which considers the portion of the trajectory that has been covered for task completion as a similarity measure. We will refer to it as the Task Completion Index (TCI). We define it in discrete form as:

$$\zeta(t_k) = \frac{\sum_{j=1}^k d(\mathbf{s}_{t_j}, \mathbf{s}_{t_{j-1}})}{\sum_{j=1}^M d(\mathbf{s}_{t_j}, \mathbf{s}_{t_{j-1}})} \quad \forall k = 1, \dots, M \quad (16)$$

where $\mathbf{s}_{t_j} \in SE(3)$ refers to the trajectory point at time instant t_j , $d(\cdot)$ to a scalar distance function and M to the total number of discrete points. Note that $0 = \zeta(t_0) \leq \zeta(t_k) \leq \zeta(t_M) = 1$. As a distance function on $SE(3)$, using the representation discussed in Section II-B, we define:

$$d(\mathbf{s}_i, \mathbf{s}_j) = \sqrt{\omega_1 [d_{\text{arc}}(\boldsymbol{\theta}_i \mathbf{u}_i, \boldsymbol{\theta}_j \mathbf{u}_j)]^2 + \omega_2 \|\mathbf{v}_i - \mathbf{v}_j\|^2} \quad (17)$$

where ω_k are a convex combination of weights for application dependent scaling and $d_{\text{arc}}(\cdot)$ is the length of the geodesic between rotations [22]:

$$d_{\text{arc}}(\boldsymbol{\theta}_i \mathbf{u}_i, \boldsymbol{\theta}_j \mathbf{u}_j) = 2 \arccos \left| \cos \frac{\theta_i}{2} \cos \frac{\theta_j}{2} + \sin \frac{\theta_i}{2} \sin \frac{\theta_j}{2} \mathbf{u}_i^T \mathbf{u}_j \right| \quad (18)$$

In Figure 3c we show that the trajectories are warped correctly, allowing then an effective encoding of the manipulation task, with the proposed TCI (Figure 3d).

D. Policy Adaptation through Via-points

The modulation of the learned policy through via-points is an important property to adapt to new situations. Let $\mathcal{V} = \{(t_i, \mathbf{s}_i^v)\}$ be the set of via-points \mathbf{s}_i^v which are desired to be reached by the policy at time instant t_i . Generalization can be implemented by conditioning the policy on both \mathcal{D} and \mathcal{V} . Assuming that the predictive distribution of each set can be computed independently, the conditioned policy is [28,29]:

$$p(\mathbf{f}^* | \mathcal{D}, \mathcal{V}, t^*) = p(\mathbf{f}^* | \mathcal{D}, t^*) p(\mathbf{f}^* | \mathcal{V}, t^*) \quad (19)$$

If $p(\mathbf{f}^* | \mathcal{D}, t^*) \sim \mathcal{N}(\boldsymbol{\mu}^d, \boldsymbol{\Sigma}^d)$ and $p(\mathbf{f}^* | \mathcal{V}, t^*) \sim \mathcal{N}(\boldsymbol{\mu}^v, \boldsymbol{\Sigma}^v)$, then, it holds that $p(\mathbf{f}^* | \mathcal{D}, \mathcal{V}, t^*) \sim \mathcal{N}(\boldsymbol{\mu}^{**}, \boldsymbol{\Sigma}^{**})$ where:

$$\boldsymbol{\mu}^{**} = \boldsymbol{\Sigma}^v (\boldsymbol{\Sigma}^d + \boldsymbol{\Sigma}^v)^{-1} \boldsymbol{\mu}^d + \boldsymbol{\Sigma}^d (\boldsymbol{\Sigma}^d + \boldsymbol{\Sigma}^v)^{-1} \boldsymbol{\mu}^v \quad (20)$$

$$\boldsymbol{\Sigma}^{**} = \boldsymbol{\Sigma}^d (\boldsymbol{\Sigma}^d + \boldsymbol{\Sigma}^v)^{-1} \boldsymbol{\Sigma}^v \quad (21)$$

The resulting distribution is computed as a product of Gaussians, and is a compromise between the via-point constraints and the demonstrated trajectories, weighted inversely by their variances. Considering an heteroscedastic GP model for \mathcal{V} (equations 10 and 11), the strength of the via-point constraints can then be easily specified by means of the latent noise function. For example, via-points with low noise will have a higher relative weight. In Figure 4 we illustrate how the distribution adapts to strong and weak defined via-points.

It should be remarked that the posterior predictive distribution of \mathcal{D} only needs to be computed once. Thus, adaptation of the policy just involves a computational cost of $\mathcal{O}(m^3)$, where m is the number of predicted outputs. Since m can be specified, the proposed approach is suitable for on-line applications (for further insight on GP complexity see [30]).

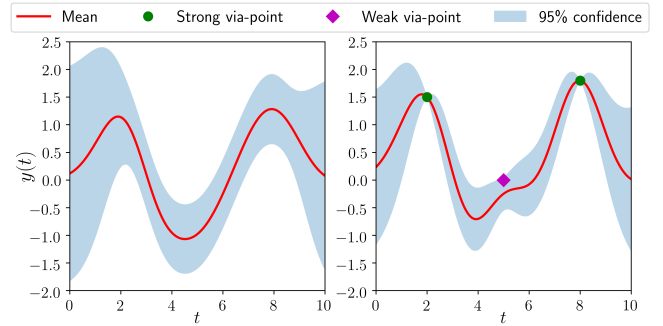


Fig. 4. On the left, a GP model based on the demonstrated trajectories. On the right, the policy adapted through via-points.

E. Modulation of the Robot Behavior

In LfD, it is often convenient to adapt the behavior of the robot as a function of the uncertainty in the different phases of the task. Let the robot end-effector be controlled through a virtual spring-mass-damper model dynamics:

$$\mathbf{M}(t) \ddot{\mathbf{e}}(t) + \mathbf{D}(t) \dot{\mathbf{e}}(t) + \mathbf{K}_p(t) \mathbf{e}(t) = \mathbf{F}_{\text{ext}}(t) \quad (22)$$

where $\mathbf{M}(t), \mathbf{D}(t), \mathbf{K}_p(t) \in \mathbb{R}^{6 \times 6}$ refer to inertia, damping and stiffness, respectively, and $\mathbf{e}(t) \in \mathbb{R}^{6 \times 1}$ is the tracking error, when subjected to an external force $\mathbf{F}_{\text{ext}}(t) \in \mathbb{R}^{6 \times 1}$.

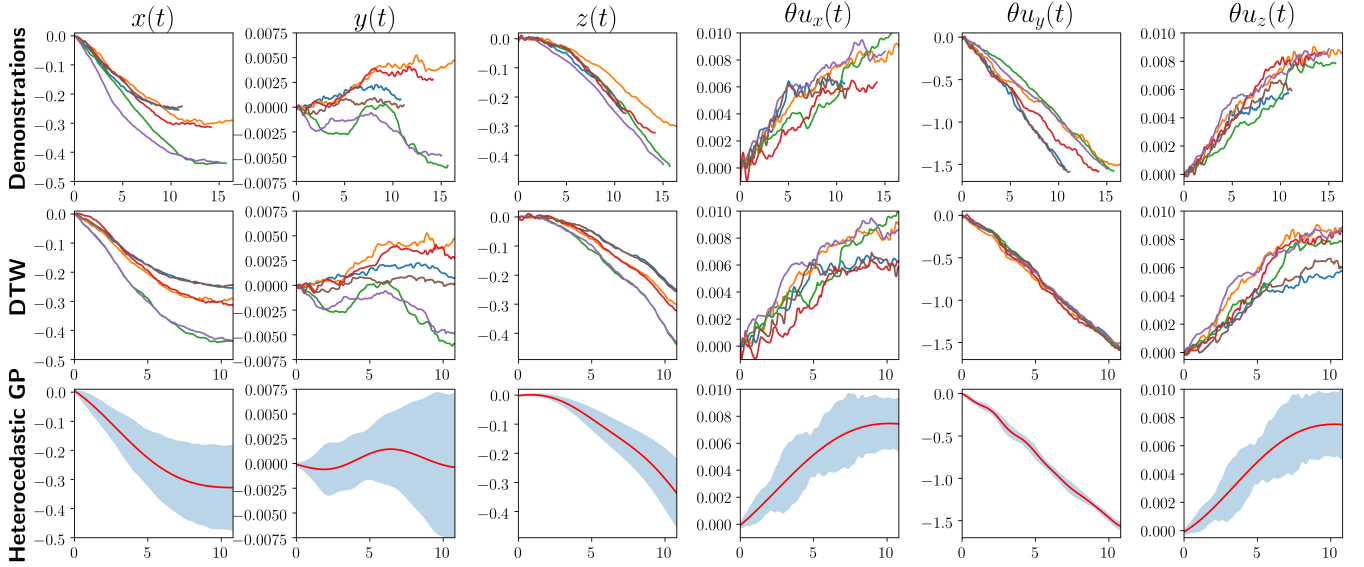


Fig. 6. In the first row, demonstrated trajectories. In the second row, alignment with DTW using TCI index. In the third row, heteroscedastic GP of each dimension of the MOGP encoding the learned policy. Note that significant variations are only observed in x , z and θu_y (see vertical axis scale).

It can be proved (see [31]) that for a constant, symmetric, positive definite \mathbf{M} , and $\mathbf{D}(t)$, $\mathbf{K}_p(t)$ continuously differentiable, the system is globally asymptotically stable if there exists a $\gamma > 0$ such that:

- 1) $\gamma\mathbf{M} - \mathbf{D}(t)$ is negative semidefinite
- 2) $\dot{\mathbf{K}}_p(t) + \gamma\dot{\mathbf{D}}(t) - 2\gamma\mathbf{K}_p(t)$ is negative definite

Now consider \mathbf{M} , $\mathbf{D}(t)$ and $\mathbf{K}_p(t)$ diagonal matrices, and a constant damping ratio δ . Substituting $d(t) = 2\delta\sqrt{mk_p(t)}$ on the second stability condition, it yields the following upper bound for the stiffness derivative:

$$\dot{k}_p(t) < \frac{2\gamma\sqrt{k_p(t)}^3}{\sqrt{k_p(t)} + 2\delta\gamma\sqrt{m}} \quad (23)$$

where m and $k_p(t)$ are an arbitrary diagonal element of \mathbf{M} and $\mathbf{K}_p(t)$, respectively. In order to modulate the robot behavior, we propose the following variable stiffness profile:

$$k_p(t) = k_p^{\max} - \frac{k_p^{\max} - k_p^{\min}}{1 + e^{-\alpha(\sigma(t) - \beta)}} \quad (24)$$

which increases the stiffness inversely to the uncertainty $\sigma(t)$ and saturates at k_p^{\min} and k_p^{\max} for high and low values respectively. Differentiating we have:

$$\dot{k}_p(t) = \alpha k_p(t) \left(1 - \frac{k_p(t)}{k_p^{\max} - k_p^{\min}} \right) \frac{d\sigma(t)}{dt} \quad (25)$$

Taking the least conservative constraints, we obtain $\gamma = 2\delta\sqrt{k_p^{\min}}$ and an upper bound of $\dot{k}_p(t)$. Then, the following sufficient stability condition can be derived:

$$\frac{d\sigma(t)}{dt} < \frac{16\delta}{\alpha} \frac{\sqrt{(k_p^{\min})^3}}{(k_p^{\max} - k_p^{\min})(1 + 4\delta^2\sqrt{m})} \quad (26)$$

The control parameters can then be tuned to satisfy the previous inequality. Note that stability is favored by high values of k_p^{\min} and small $k_p^{\max} - k_p^{\min}$ and α .

IV. AN EXAMPLE APPLICATION: DOOR OPENING TASK

In order to illustrate how the proposed GP-based LfD approach can be applied to real-world manipulation tasks, we address the problem of opening doors using a TIAGo robot. This is a relevant skill for robots assisting people in domestic environments [32].

A. Policy Inference from Human Demonstrations

We performed human demonstrations using an Xsens MVN motion capture system. Right hand trajectories of the human teacher relative to the initial closed door position were recorded for three different doors (Figure 5). Coordinate axes were chosen such as the pulling direction is parallel to the x axis and the y axis is perpendicular to the floor. The demonstration dataset consisted in a total of 6 trajectories, two per each door.



Fig. 5. Demonstrations were recorded using an Xsens MVN motion capture system. The teacher opens three doors with different radius.

The recorded trajectories were then temporally aligned using DTW and the proposed TCI index. Next, the data was used to infer the door opening policy. In Figure 6 we show these steps for each output dimension. On the third row, we can see the resulting heteroscedastic MOGP representation. Note that in the door opening motion, significant variations are only observed in the x , z and θu_y components. We can see that the trajectories are warped effectively using the proposed TCI similarity measure, since they are clearly clustered in three groups, one for each type of door.

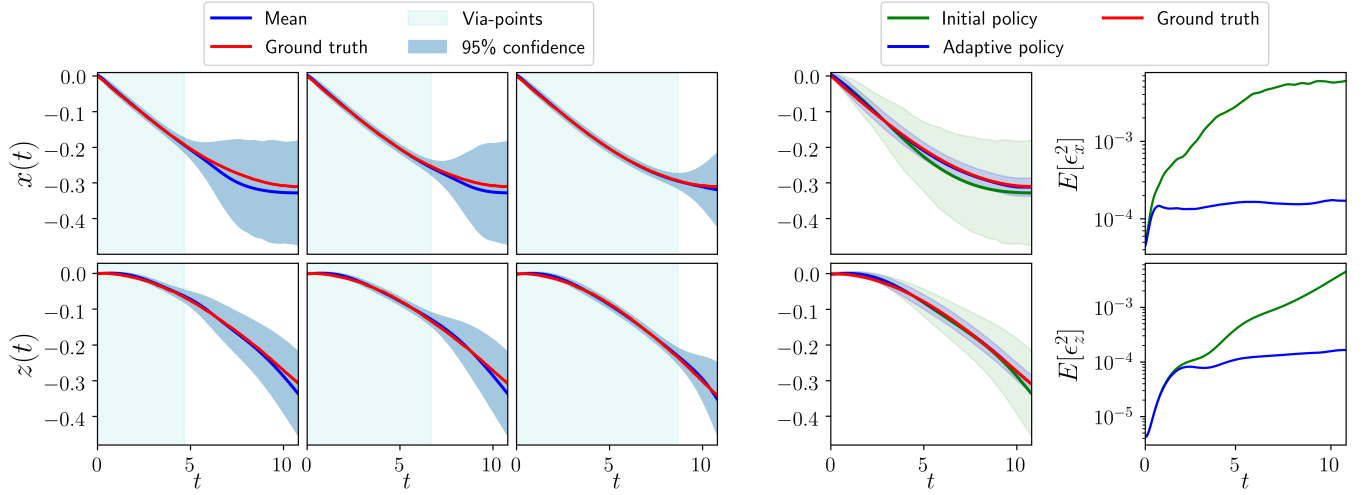


Fig. 9. The first three columns show how does the posterior distribution vary considering as via-points the observations of the door motion in the light-blue shaded area. The next column shows the comparison between the predictive distribution considering the adaptive policy or the policy based only on human demonstrations. The shaded areas and lines of the same color correspond to the 95% confidence interval and mean, respectively. The column on the right shows the mean squared prediction error of each policy.

It can also be observed that the resulting heteroscedastic MOGP effectively encodes the skill. This is more evident in Figure 7, where position uncertainty has been projected onto the $x-z$ plane. We can observe the uncertainty in the door radius is accurately captured from demonstrations.

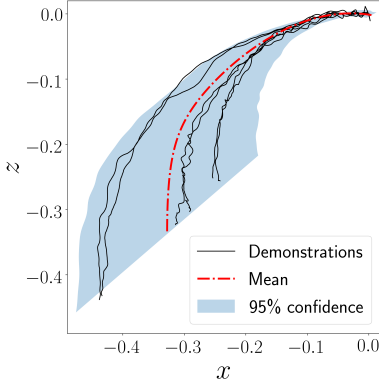


Fig. 7. Door opening policy projected on the $x-z$ plane.

B. Policy Adaptation and Modulation of the Robot Behavior

In the reproduction stage, we gather observations of the door motion solving the forward kinematics of the robot. These observations can then be defined as via-points to improve the policy prediction capabilities. Additionally, we can take advantage of the forces exerted by the door to correct small biases on the policy, adopting a variable admittance control scheme. The set-point of the controller is changed through the virtual dynamics discussed in Section III-E.



Fig. 8. TIAGo robot opening the door.

With the proposed approach we successfully performed the door opening task with TIAGo (Figure 8). We can see in Figure 9, on the first three columns on the left, how the posterior distribution varies for coordinates x and z as the door is opened. We show that the adaptive policy converges to the ground truth trajectory. On the next column, we show the comparison between the resulting distribution at step t_i considering via-points up to t_{i-1} , and the initial policy. In order to obtain a quantitative measure of the prediction performance, we evaluated the mean squared prediction error, $E[\epsilon^2] = (E[f^*(t^*)] - f(t^*))^2 + \text{var}[f^*(t^*)]$. We can observe that the adaptive policy clearly achieves a better performance.

The resulting variable stiffness profile is shown in Figure 10. We have tuned the parameters empirically, being the used values $k_p^{max} = 500$, $k_p^{min} = 100$, $m = 1$, $\delta = 1$, $\alpha = 600$ and $\beta = 0.01$. For simplicity, we have considered the same law for the 6 degrees of freedom. We can observe that the robot behavior is modulated towards a more compliant behavior towards the final phases, where the policy is more uncertain. We can also see that the stability bound is not crossed, which is coherent with the behavior observed in the conducted experiments, where no instabilities occurred.

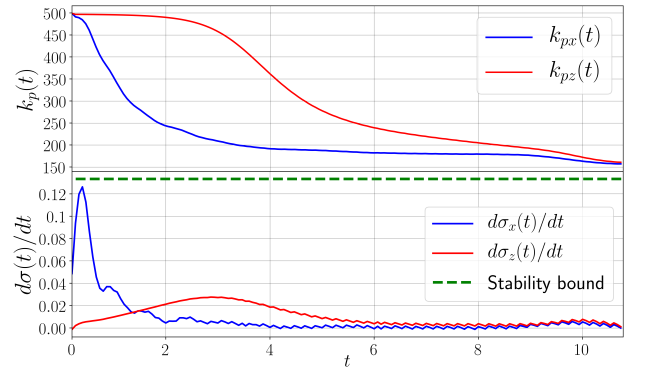


Fig. 10. On top, variable stiffness profile for x and z . Below, the evolution of the uncertainty derivative of the adaptive policy.

V. CONCLUSION

Gaussian Processes (GP) are a promising paradigm for learning manipulation skills from human demonstrations. In this paper, we present a novel approach that takes advantage of the versatility and expressiveness of these models to encode task policies. We propose an heteroscedastic multi-output GP policy representation, inferred from demonstrations. This model considers a suitable parametrization of task space rotations for GP and ensures that only continuous and smooth paths are generated. Furthermore, the introduction of an input-dependent latent noise function allows an effective simultaneous encoding of the prediction uncertainty and the variability of demonstrated trajectories.

In order to effectively establish a correlation between temporal and spatial coordinates, demonstrations must be aligned. This operation can be performed with the Dynamic Time Warping algorithm. We introduce the novel Task Completion Index, a similarity measure that allows to achieve an effective warping when the learned task requires the consideration of different paths. Adaptation of the policy can be performed by conditioning it on a set of specified via-points. We also introduce a new computationally efficient method, where the relative importance of the constraints can also be defined. Additionally, we propose an innovative variable stiffness profile that takes advantage of the uncertainty measure provided by the GP model to stably modulate the robot end-effector dynamics.

We illustrated the proposed learning from demonstration framework through the door opening task and evaluated the performance of the learned policy through real-world experiments with the TIAGo robot. Results show that the manipulation skill is effectively encoded and a successful reproduction can be achieved taking advantage of the presented policy adaptation and robot behavior modulation approaches.

This work aims to push the state-of-the-art in learning from demonstration towards easily extending robot capabilities. Future research will be conducted focusing on its applicability on complex tasks, such as cloth manipulation.

REFERENCES

- [1] A. Colomé and C. Torras, *Reinforcement Learning of Bimanual Robot Skills*. Springer Tracts in Advanced Robotics (STAR), vol. 134. Springer International Publishing, 2020.
- [2] H. Ravichandar, A. Polydoros, S. S. Chernova, and A. Billard, "Recent advances in robot learning from demonstration," *Annual Review of Control, Robotics, and Autonomous Systems*, vol. 3, May 2020.
- [3] S. Calinon, "A tutorial on task-parameterized movement learning and retrieval," *Intelligent Service Robotics*, vol. 9, no. 1, Jan 2016.
- [4] E. Pignat and S. Calinon, "Bayesian Gaussian Mixture Model for robotic policy imitation," *IEEE Robotics and Automation Letters (RA-L)*, vol. 4, no. 4, pp. 4452–4458, 2019.
- [5] A. J. Ijspeert, J. Nakanishi, and S. Schaal, "Trajectory formation for imitation with nonlinear dynamical systems," in *Proceedings 2001 IEEE/RSJ International Conference on Intelligent Robots and Systems*, vol. 2, Oct 2001, pp. 752–757.
- [6] P. Pastor, H. Hoffmann, T. Asfour, and S. Schaal, "Learning and generalization of motor skills by learning from demonstration," in *2009 IEEE International Conference on Robotics and Automation*, May 2009, pp. 763–768.
- [7] A. Paraschos, C. Daniel, J. Peters, and G. Neumann, "Using probabilistic movement primitives in robotics," *Autonomous Robots*, vol. 42, no. 3, pp. 529–551, March 2018.
- [8] M. Ewerton, O. Arenz, G. Maeda, D. Koert, Z. Kolev, M. Takahashi, and J. Peters, "Learning trajectory distributions for assisted teleoperation and path planning," *Frontiers in Robotics and AI*, vol. 6, 2019.
- [9] Y. Huang, L. Roza, J. Silvério, and D. Caldwell, "Kernelized Movement Primitives," *The International Journal of Robotics Research*, vol. 38, no. 7, pp. 833–852, 2019.
- [10] G. Camps-Valls, J. Verrelst, J. Muoz-Marí, V. Laparra, F. Mateo-Jiménez, and J. Gómez-Dans, "A Survey on Gaussian Processes for Earth-Observation Data Analysis: A Comprehensive Investigation," *IEEE Geoscience and Remote Sensing Magazine*, vol. 4, no. 2, 2016.
- [11] E. Schulz, M. Speekenbrink, and A. Krause, "A tutorial on Gaussian Process regression: Modelling, exploring, and exploiting functions," *Journal of Mathematical Psychology*, vol. 85, pp. 1–16, 2018.
- [12] C.-E. Rasmussen and C.-K.-I. Williams, *Gaussian Processes for Machine Learning*. The MIT Press, 2006.
- [13] C.-M. Bishop and J. Lasserre, "Generative or Discriminative? Getting the best of both worlds," in *Bayesian Statistics 8*, J.-M. Bernardo, M.-J. Bayarri, J.-O. Berger, A.-P. Dawid, D. Heckerman, A.-F. Smith, and M. West, Eds. International Society for Bayesian Analysis, 2007.
- [14] D. Nguyen-Tuong and J. Peters, "Local Gaussian Process regression for real-time model-based robot control," in *2008 IEEE/RSJ International Conference on Intelligent Robots and Systems*, Sept 2008.
- [15] D. Forte, A. Ude, and A. Kos, "Robot learning by Gaussian Process regression," in *19th International Workshop on Robotics in Alpe-Adria-Danube Region (RAAD 2010)*, June 2010, pp. 303–308.
- [16] M. Schneider and W. Ertel, "Robot learning by demonstration with local Gaussian Process regression," in *2010 IEEE/RSJ International Conference on Intelligent Robots and Systems*, Oct 2010.
- [17] N. Jaquier, D. Ginsbourger, and S. Calinon, "Learning from demonstration with model-based Gaussian Process," in *3rd Conference on Robot Learning (CoRL)*, Osaka, Japan, Oct 2019.
- [18] K.-P. Murphy, *Machine Learning: A Probabilistic Perspective*. The MIT Press, 2012.
- [19] M.-A. Álvarez, L. Rosasco, and N.-D. Lawrence, "Kernels for vector-valued functions: A review," *Foundations and Trends in Machine Learning*, vol. 4, no. 3, pp. 195–266, Mar 2012.
- [20] H. Liu, J. Cai, and Y.-S. Ong, "Remarks on Multi-Output Gaussian Process Regression," *Knowledge-Based Systems*, vol. 144, pp. 102–121, March 2018.
- [21] M. Lang, M. Kleinstueber, and S. Hirche, "Gaussian Process for 6-DoF rigid motions," *Autonomous Robots*, vol. 42, no. 6, 2018.
- [22] M. Lang and S. Hirche, "Computationally efficient rigid-body Gaussian Process for motion dynamics," *IEEE Robotics and Automation Letters*, vol. 2, no. 3, pp. 1601–1608, July 2017.
- [23] P. Goldberg, C. Williams, and C. Bishop, "Regression with input-dependent noise: A Gaussian Process treatment," *Advances in Neural Information Processing Systems*, vol. 10, pp. 493–499, Jan 1998.
- [24] K. Kersting, C. Plagemann, P. Pfaff, and W. Burgard, "Most-likely Heteroscedastic Gaussian Process regression," in *ACM International Conference Proceeding Series*, vol. 227, Jan 2007, pp. 393–400.
- [25] R. Bellman and R. Kalaba, "On adaptive control processes," *IRE Transactions on Automatic Control*, vol. 4, no. 2, pp. 1–9, Nov 1959.
- [26] P. Senin, "Dynamic Time Warping algorithm review," Information and Computer Science Department, University of Hawaii at Manoa, Honolulu, USA, Tech. Rep., Dec 2008.
- [27] A. Vakanski, I. Mantegh, A. Irish, and F. Janabi-Sharifi, "Trajectory learning for robot programming by demonstration using Hidden Markov Model and Dynamic Time Warping," *IEEE Transactions on Systems, Man, and Cybernetics, Part B (Cybernetics)*, vol. 42, no. 4, pp. 1039–1052, Aug 2012.
- [28] M. Deisenroth and J.-W. Ng, "Distributed Gaussian Processes," in *32nd International Conference on Machine Learning (ICML)*, vol. 37, July 2015, pp. 1481–1490.
- [29] H. Liu, Y. Ong, X. Shen, and J. Cai, "When Gaussian Process meets big data: A review of scalable GPs," *IEEE Transactions on Neural Networks and Learning Systems*, pp. 1–19, 2020.
- [30] H.-L. Bilj, "LQG and Gaussian Process Techniques for Fixed-Structure Wind Turbine Control," PhD Dissertation, Delft University of Technology, The Netherlands, Tech. Rep., Oct 2018.
- [31] K. Kronander and A. Billard, "Stability considerations for variable impedance control," *IEEE Transactions on Robotics*, vol. 32, no. 5, pp. 1298–1305, Oct 2016.
- [32] D. Kim, J.-H. Kang, C.-S. H. CS., and G.-T. Park, "Mobile robot for door opening in a house," in *Knowledge-Based Intelligent Information and Engineering Systems (KES), Part II*, Sept 2004, pp. 596–602.